

Isolation and Characterization of Borane Complexes of Dimethylsulfoxonium Methylide

J. M. Stoddard and K. J. Shea*

Department of Chemistry, University of California, Irvine, California

Received October 15, 2002

Trialkylboranes (R_3B) catalyze the repetitive insertion of methylene from dimethylsulfoxonium methylide (**1**) to form polymethylene. A proposed intermediate in this reaction is a 1:1 complex between R_3B and ylide **1**. Following complexation, an alkyl group (boron-substituted) undergoes a 1,2-migration to the methylide carbon with displacement of a molecule of DMSO. A series of complexes of dimethylsulfoxonium methylide (**1**) and various organoboranes, X_3B ($X = H, Ph, F, C_6F_5$), have been prepared and isolated. Molecular structures, obtained by single-crystal X-ray diffraction, for ylide· BF_3 (**3**) and ylide· $B(C_6F_5)_3$ (**4**) were found to contain geometries with potential migrating groups anti-periplanar to the carbon–sulfur bond. The stability of solutions of these complexes ranges considerably. For example, ylide· BPh_3 (**6**) undergoes reaction at room temperature, while ylide· $B(C_6F_5)_3$ (**3**) is stable to temperatures > 100 °C. All complexes can be prepared as solids stable at room temperature. The solid-state stability of ylide· BR_3 complexes was evaluated by differential scanning calorimetry. The decomposition temperature increases across the series for $R = H, Ph, C_6F_5, F$. The heats of reaction of ylide· BR_3 are $R = H$ (–54.7), Ph (–15.7), C_6F_5 (–21.6), and F (–17.1) kcal mol^{–1}, respectively.

Introduction

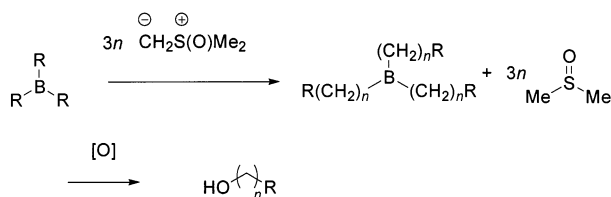
Organoborane chemistry has played an important role in the construction of carbon–carbon bonds.^{1,2} Many of these reactions involve formation of a tetrahedral “ate” complex followed by transfer of a carbon nucleophile to an acceptor. The transfer can be intermolecular, such as in the Suzuki reaction,^{3,4} or intramolecular.^{5,6} Examples of the latter include reactions of trialkylboranes with nucleophilic reagents such as ethyl bromoacetate,⁷ α -chloroacetonitrile,⁷ α -bromo ketones,⁸ dihalomethyl-lithium,⁹ dimethylsulfoxonium methylide (**1**),^{10,11} dimethylsulfonium methylide (**2**),¹² and various diazo compounds.^{13–16} These reactions result in formation of new carbon–carbon bonds, and several have achieved synthetic utility. Dimethylsulfoxonium methylide (**1**) coordinates to a variety of metals including Au, Be, Al,

Ga, In, Ni, Pd, Cr, and Mo.^{17–20} These ylide-metal complexes, however, do not undergo simple rearrangement as do the triorganoboranes. Organoboranes also form complexes with phosphonium ylides, which undergo subsequent 1,2-migration at elevated reaction temperatures.²¹ Recently, trialkylboranes have been found to react with dimethylsulfoxonium methylide (**1**) (Scheme 1),^{22–28} resulting in multiple insertions of methylene into the carbon–boron bond. The reaction produces polymethylene, a linear hydrocarbon polymer comprised of repeating CH_2 units. It has been proposed that the polyhomologation involves a reaction cycle that includes the formation of a 1:1 complex between R_3B and ylide **1** (Scheme 2). Subsequent 1,2-migration by an alkyl group affords a homologated organoborane and dimethyl sulfoxide. The organoborane product re-enters the cycle to produce eventually a tris-polymethylene borane. Subsequent oxidation affords ω -hydroxypoly-methylene (Scheme 1).

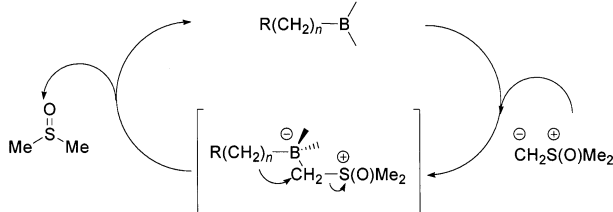
- (1) Matteson, D. S. *Chem. Rev.* **1989**, *89*, 1535–1551.
 (2) Weill-Raynal, J. *Synthesis* **1976**, 633–651.
 (3) Chemler, S. R.; Trauner, D.; Danishefsky, S. J. *Angew. Chem., Int. Ed.* **2001**, *40*, 4544–4568.
 (4) Miyaura, N.; Suzuki, A. *Chem. Rev.* **1995**, *95*, 2457–2483.
 (5) Brown, H. C. *Organic Synthesis via Borane*; Wiley-Interscience: New York, 1975.
 (6) Mikhailov, B. M.; Bubnov, Y. N. *Organoboron Compounds in Organic Synthesis*; Harwood Academic Publishers GmbH: Switzerland, 1984.
 (7) Brown, H. C.; Nambu, H.; Rogic, M. M. *J. Am. Chem. Soc.* **1969**, *91*, 6855.
 (8) Brown, H. C.; Rogic, M. M.; Rathke, M. W. *J. Am. Chem. Soc.* **1968**, *90*, 6218.
 (9) Matteson, D. S. *Tetrahedron* **1998**, *54*, 10555.
 (10) Tufariello, J.; Lee, L. *J. Am. Chem. Soc.* **1966**, *88*, 4757.
 (11) Tufariello, J.; Lee, L.; Wotjkowski, P. *J. Am. Chem. Soc.* **1967**, *89*, 6804.
 (12) Tufariello, J.; Wotjkowski, P.; Lee, L. *J. Chem. Soc., Chem. Commun.* **1967**, 10, 505.
 (13) Hooz, J.; Linke, S. *J. Am. Chem. Soc.* **1968**, *90*, 6891.
 (14) Hooz, J.; Gunn, D. M. *J. Am. Chem. Soc.* **1969**, *91*, 6195.
 (15) Hooz, J.; Morrison, G. F. *Can. J. Chem.* **1970**, *48*, 868.
 (16) Seyferth, D. *Chem. Rev.* **1955**, *55*, 1155.

- (17) Yamamoto, Y. *Bull. Chem. Soc. Jpn.* **1987**, *60*, 1189–1191.
 (18) Poerschke, K. R. *Chem. Ber.* **1987**, *120*, 425–427.
 (19) Lin, I. J. B.; Lai, H. Y. C.; Wu, S. C.; Hwan, L. *J. Organomet. Chem.* **1986**, *306*, C24–C26.
 (20) Weber, L. *Z. Naturforsch., B: Anorg. Chem., Org. Chem.* **1976**, *31B*, 780–785.
 (21) Bestmann, H. J.; Roeder, T.; Suehs, K. *Chem. Ber.* **1988**, *121*, 1509–1517.
 (22) Shea, K. J.; Busch, B. B.; Paz, M. M.; Staiger, C. L.; Stoddard, J. M.; Walker, J. R.; Zhou, X.; Zhu, H. *J. Am. Chem. Soc.* **2002**, *124*, 3636.
 (23) Shea, K. J.; Wagner, C. E. *Org. Lett.* **2001**, *3*, 3063.
 (24) Shea, K. J.; Zhou, X.-Z. *J. Am. Chem. Soc.* **2000**, *122*, 11515.
 (25) Shea, K. J.; Lee, S. Y.; Busch, B. B. *J. Org. Chem.* **1998**, *63*, 5746.
 (26) Shea, K. J. *Chem. Eur. J.* **2000**, *6*, 1113.
 (27) Shea, K. J.; Busch, B. B.; Paz, M. M. *Angew. Chem., Int. Ed.* **1998**, *38*, 1391.
 (28) Shea, K. J.; Zhu, H.; Walker, J. R.; Paz, M. M.; Greaves, J. J. *Am. Chem. Soc.* **1997**, *119*, 9049.

Scheme 1



Scheme 2



We are interested in the structure, stability, and activation energy for the subsequent 1,2-migration of the proposed intermediate, a zwitterionic complex. Screening studies of Lewis acidic catalysts for the polyhomologation reaction have revealed significant differences in reactivity of the ylide-borane complex.²⁹ In an effort to design more efficient catalysts, we wished to understand how boron substituents influence the stability of the complex and the activation energy for the subsequent reaction. We report the synthesis and isolation of complexes of ylide **1** and boranes. These complexes are crystalline solids that exhibit a range of thermal stabilities. The quantification of their stability by thermal analysis has provided an opportunity to evaluate the influence of substituents on boron on the activation energy for subsequent reactions.

Results and Discussion

At low temperatures, trialkylboranes form 1:1 complexes with ylide **1**. Upon warming to room temperature, they readily undergo 1,2-migration to produce homologated organoboranes. Alkylboronic and alkylborinic esters also form 1:1 complexes with ylide **1** (¹¹B NMR). However these complexes do not decompose to form the corresponding homologated organoboranes, even at elevated temperatures.²⁹ Additional studies confirmed that the stability of ylide-borane complexes was sensitive to substituents on boron. For example, $BH_3 \cdot SME_2$ and Ph_3B were efficient initiators for polyhomologation at 23 °C, while $BF_3 \cdot OEt_2$ and $B(C_6F_5)_3$ were ineffective, even at temperatures up to 100 °C. It is assumed that in all cases coordination of ylide **1** with the Lewis acidic organoborane takes place, but 1,2-migration does not occur in the two latter cases. To obtain support for this proposal, we first investigated the BF_3 and $B(C_6F_5)_3$ complexes of ylide **1** since they are ineffective at bringing about polyhomologation at room temperature.

The addition of $BF_3 \cdot OEt_2$ to a solution of ylide **1** in toluene at room temperature produced a precipitate that was filtered and recrystallized from $EtOH/H_2O$ to afford analytically pure ylide- BF_3 complex **3**³⁰ in 50% yield. The solution ¹⁹F NMR (1:1 $MeOH-d_4/d_2O$) shows a quartet at 134.5 ppm ($J_{F-B} = 45$ Hz), and the ¹¹B NMR

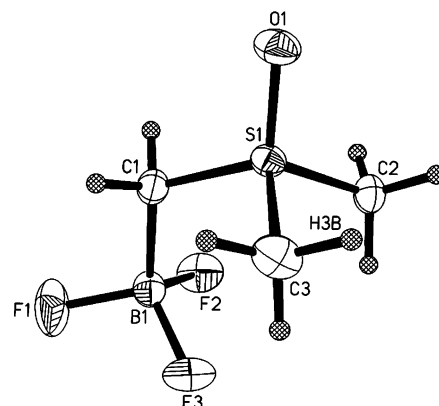


Figure 1. Molecular structure of **3**. Selected bond lengths (Å) and angles (deg): S1–C1 1.742(1), S1–C3 1.761(2), S1–C2 1.758(2), S1–O1 1.454(1), C1–B1 1.650(2) F1–B1 1.394(2), F2–B1 1.400(2), F3–B1 1.400(2); C1–S1–C2 108.11(7), C1–S1–C3 106.88(7), C1–S1–O1 113.22(7), C2–S1–C3 105.43(8), C3–S1–O1 111.06(8), C2–S1–O1 111.72(7), C1–B1–F1 107.97(11), C1–B1–F2 110.38(12), C1–B1–F3 112.45(11), F1–B1–F2 109.24(12), F1–B1–F3 108.70(14), F2–B1–F3 108.05(12).

shows a quartet at –23 ppm ($J_{B-F} = 45$ Hz). Typical ¹¹B chemical shifts for trigonal boranes range from 90 to 25 ppm, while tetrahedral borates range from 0 to –20 ppm.³¹ The observed ¹¹B chemical shift for complex **3** is consistent with a borate complex.

The molecular structure of complex **3**, obtained by single-crystal X-ray analysis, is shown in Figure 1. The complex has a staggered conformation about the B1–C1 bond with an alignment one of the fluorine atoms anti to the sulfoxonium group ($F1-B1-C1-S1 = -161.21(11)^\circ$). The anti fluorine has a slightly shorter B–F distance (1.394 Å) compared to the two remaining fluorines (1.400 Å). In addition, the $F1-B1-C1$ angle ($107.97(11)^\circ$) is smaller than the two remaining $F3-B1-C1$ ($112.45(11)^\circ$) and $F2-B1-C1$ ($110.38(12)^\circ$) angles. The sulfur–oxygen bond of complex **3** is aligned anti to the B–C bond ($B1-C1-S1-O1 166.42(10)^\circ$), which may be due to the opposing dipole moments of the BF_3 and S–O groups.

The ylide- $B(C_6F_5)_3$ (**4**) complex was prepared by the addition of a solution of ylide **1** in toluene to a solution of tris(pentafluorophenyl)borane in toluene. The solvent was evaporated to afford a white solid, which was crystallized from $CHCl_3$ /hexanes to afford complex **4** in 82% yield. The ¹¹B NMR of tris(pentafluorophenyl)borane in toluene-*d*₆ shows a broad singlet at 59.8 ppm. Complex **4**, however, exhibits a sharp singlet at –17.8 ppm consistent with a tetrahedral borane. The ¹⁹F NMR shows three resonances consistent with ortho (133.2 ppm), meta (158.8 ppm), and para (164.3 ppm) fluorines of complex **4**.

The molecular structure of complex **4**, obtained by single-crystal X-ray analysis, is shown in Figure 2. The substituents on B1 and C19 are staggered, and one of the aryl rings is aligned anti to the C19–S1 bond ($C1-B1-C19-S1 = 165.4(2)^\circ$). The aligned aryl ring has a longer B–C bond distance ($B1-C1 = 1.664(3)$ Å) compared to the remaining aryl groups (1.655(3), 1.648(3) Å). In contrast to the ylide- BF_3 complex **3**, the sulfur–oxygen bond of complex **4** is aligned gauche to the B–C

(29) Unpublished results.

(30) Corey, E. J.; Chaykovsky, M. *J. Am. Chem. Soc.* **1965**, *87*, 1353.

(31) Wrackmeyer, B. *Annu. Rep. NMR Spectrosc.* **1988**, *20*, 61.

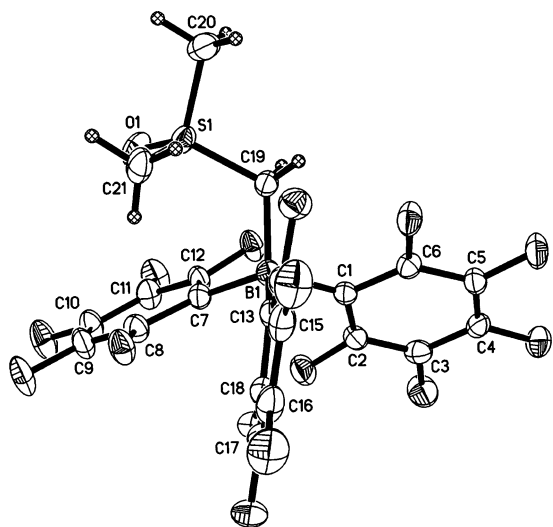


Figure 2. Molecular structure of **4**. Selected bond lengths (Å) and bond angles (deg): S1–C19 1.756(2), S1–C21 1.755(2), S1–C20 1.753(3), S1–O1 1.438(2), C19–B1 1.674(3), B1–C1 1.664(3), B1–C7 1.655(3), B1–C13 1.648(3); C19–S1–O1 113.88(11), C19–S1–C21 109.94(11), C19–S1–C20 105.90(12), C20–S1–C21 104.19(14), C21–S1–O1 111.33(12), C20–S1–O1 111.04(12), S1–C19–B1 118.65(15), C19–B1–C1 105.33(16), C19–B1–C7 105.69(17), C19–B1–C13 115.05(18), C1–B1–C7 113.76(18), C1–B1–C13 104.03(16), C7–B1–C13 112.95(17).

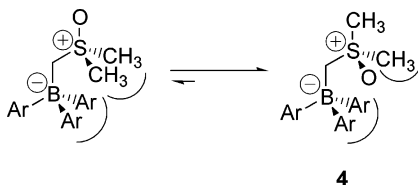


Figure 3. Complex ylide·B(C₆F₅)₃ (**4**) prefers the gauche conformation. Diminished steric interactions between the aryl groups and sulfoxonium methyls may contribute to the preference.

bond (B1–C19–S1–O1 = 69.7(2)°). This may be due to steric interactions between the two sulfoxonium methyls and aryl rings (Figure 3). The proximity between the electron-rich sulfoxonium oxygen and one of the electron-deficient aromatic rings (3.075 Å) in structure **4** could also contribute to the observed geometry.

Complex **4** contains two geared aryl rings, while a third aryl ring is synclinal to the ylide carbon–boron bond (C19–B1–C1–C6 = 53.7(2)°). The aryl C–B bond is aligned anti-periplanar to the C–S bond. The twisted conformation of the aryl ring allows favorable orbital overlap between the aromatic π -system (HOMO) and the C–S σ^* (LUMO) (Figure 4b). This orientation is also preferred in the related pinacol and Wagner–Meerwein shifts of phenyl rings.³²

Borane initiates the polymerization of ylide **1** at room temperature. Therefore, the attempted preparation of its complex was carried out at –40 °C. A solution of ylide **1** in THF was added to an equimolar amount of BH₃·SMe₂ in THF at –40 °C. A white precipitate formed within 10 min. The precipitate was filtered cold, washed with cold hexane, and dried in vacuo to afford ylide·BH₃ (**5**) in quantitative yield.³³ As a microcrystalline solid, complex **5** could be handled routinely at room

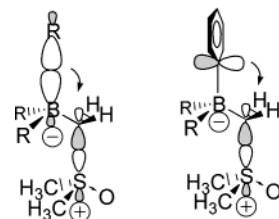


Figure 4. (a) Proposed molecular orbital interactions favor the migrating group (HOMO: C–B σ) to align anti-periplanar to the sulfoxonium leaving group (LUMO: C–S σ^*). (b) Preferred orientation of aryl ring with aromatic π -system aligned with C–S σ^* .

temperature without apparent decomposition. However, when samples were stored in screw-cap vials at room temperature, colorless crystals formed near the cap. A single-crystal X-ray analysis identified the substance as methylboronic acid, apparently formed by 1,2-migration of complex **5** followed by reaction with adventitious water. To avoid this, samples were stored at –20 °C for prolonged periods of time without apparent decomposition. The complex **5** was sparingly soluble in DMF at 0 °C. The ¹¹B NMR indicated a sharp singlet at –31.2 ppm. The IR spectrum shows a characteristic B–H stretching frequency at 2284 cm^{–1} consistent with a monomeric hydridoborate species.³⁴

Triphenylborane is also an efficient initiator for the polymerization of **1** at room temperature; therefore a low-temperature synthesis of the ylide complex with triphenylborane was employed. The addition of an equimolar amount of ylide **1** in THF to a solution of triphenylborane in THF at –78 °C afforded a homogeneous solution of ylide·BPh₃ (**6**). The ¹¹B NMR (CDCl₃) of triphenylborane shows a broad singlet at 67.0 ppm, while ylide·BPh₃ complex **6** in toluene-*d*₈ at –40 °C shows a sharp singlet at –10.3 ppm. The ¹¹B chemical shift is consistent with the tetrahedral borate of complex **6**.³¹

Efforts to obtain single crystals suitable for X-ray analysis of complex **6** by slowly removing the solvent in vacuo at –40 °C resulted in the formation of a microcrystalline solid. Interestingly, after solvent removal at low temperatures (–40 °C), solid complex **6** was stable at room temperature and could be stored at room temperature without decomposition for more than six months. The solid-state stability of this complex must reflect restricted motion along a reaction coordinate imposed by the crystal lattice.³⁵

A microcrystalline sample of complex **6** was heated to 90 °C for 10 min, then oxidized with trimethylamine-*N*-oxide in THF at room temperature for 3 h. The product mixture was analyzed by GC/MS and found to contain the following amounts of phenol (57%), benzyl alcohol (42%), and phenethyl alcohol (<1%).

Thermal Analyses of Ylide-Borane Complexes 3–6. Although all solid complexes were stable at room temperature, the onset temperature at which a solid-state reaction took place varied considerably. It was

(33) Caution, The BH₃-ylide complex has been prepared in 3 g quantities as a white solid substance. The DSC (<1.5 mg) shows a very exothermic transition above 55 °C, and larger amounts of solid complex should not be heated.

(34) Golthup, M.; Daly, L.; Wiberey, S. *Introduction to Infrared and Raman Spectroscopy*, S. 292; Academic Press: New York/London, 1990.

(35) Boldyrev, V. V. *React. Solids* **1990**, *8*, 231–246.

(32) Bachmann, W.; Gerguson, J. *J. Am. Chem. Soc.* **1934**, *56*, 2081.

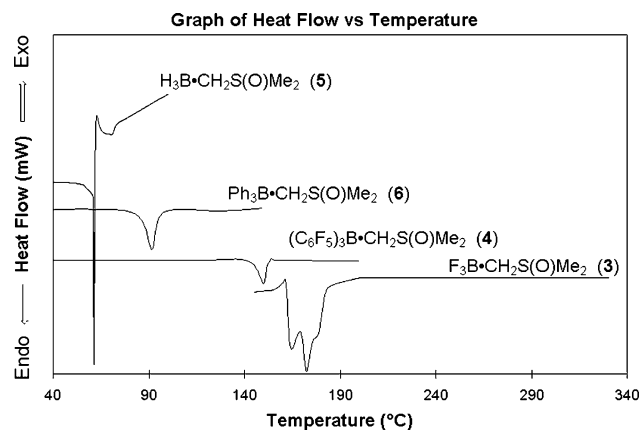


Figure 5. DSC traces of complexes **3–6** at $10\text{ }^{\circ}\text{C min}^{-1}$ and arbitrary y -offset

Table 1. Thermodynamic Data for Complexes **3–6**^a

compound	ΔH_{rxn}	ΔH_{m}	T_{d} at $5\text{ }^{\circ}\text{C min}^{-1}$	T_{on} at $5\text{ }^{\circ}\text{C min}^{-1}$
$\text{F}_3\text{B}\cdot\text{ylide (3)}$	-11.3	1.6	157.3–185.2	157.3
$(\text{C}_6\text{F}_5)_3\text{B}\cdot\text{ylide (4)}$	-21.6	0.4	144.5–153.5	144.5
$\text{BH}_3\cdot\text{ylide (5)}$	-54.7	0.1	60.9–62.4	60.9
$\text{Ph}_3\text{B}\cdot\text{ylide (6)}$	-15.7	0.3	88.0–96.5	88.0

^a Heats of reaction in kcal mol^{-1} , temperature in $^{\circ}\text{C}$. ΔH_{rxn} and ΔH_{m} are the nonreversing (1,2-migration) and reversing (melting) heat flow, respectively, from MDSC. T_{d} is the exothermic range and T_{on} is the onset temperature of reaction from DSC.

decided to quantitate these differences using thermal analyses of the solids. Reactions in the melt or solution can generally be described by Arrhenius kinetics. In contrast, physical characteristics (dislocations, crystal size, nuclei distribution, etc.) play a roll in the kinetic equations that describe solid-state reactions.³⁶ These reactions are referred to as topochemical reactions and occur in the solid state with the least amount of molecular motion.³⁵ The neighboring molecules in the crystal lattice largely determine the course and stereochemistry of these reactions. Differences between the solid-state and solution reactions are well documented. For example, the kinetics of the thermal *cis* to *trans* isomerization of azobenzene has been studied in the solid and melt. The Arrhenius parameters in the solid state ($E_{\text{a}} = 53.3\text{ kcal mol}^{-1}$, $\log A = 31.04$) are substantially higher than the melt ($E_{\text{a}} = 24.7\text{ kcal mol}^{-1}$, $\log A = 12.21$).³⁷ It is reasonable therefore to expect the solid-state lattice energy to stabilize otherwise labile, reactive ylide-borane complexes.

Differential scanning calorimetry (DSC) was employed to evaluate the thermochemistry of reaction. An overlay of the DSC scans of the four complexes is shown in Figure 5. Most crystalline solids display an endotherm upon melting; however all the ylide-borane complexes exhibit an exothermic peak, presumably due to the exothermicity associated with reaction superimposed on the melting exotherm. The onset temperatures for the exothermic peak for complexes **3–6** are listed in Table 1. With a scan rate of $5\text{ }^{\circ}\text{C min}^{-1}$ these vary from $60.9\text{ }^{\circ}\text{C}$ for $\text{BH}_3\cdot\text{ylide (5)}$ to $157.3\text{ }^{\circ}\text{C}$ for $\text{BF}_3\cdot\text{ylide (3)}$.

(3). The exothermic peak width for $\text{BH}_3\cdot\text{ylide (5)}$ is very sharp³⁴ ($<2\text{ }^{\circ}\text{C}$), whereas the peak widths for $\text{B}(\text{C}_6\text{F}_5)_3\cdot\text{ylide (4)}$ and $\text{BPh}_3\cdot\text{ylide (6)}$ are less so ($<10\text{ }^{\circ}\text{C}$). In contrast the DSC scan for $\text{BF}_3\cdot\text{ylide (3)}$ shows a slight endothermic peak preceding two exothermic peaks with a much broader temperature range ($\sim 30\text{ }^{\circ}\text{C}$). In an effort to identify the products of decomposition, complex **3** was gradually heated to $200\text{ }^{\circ}\text{C}$ and continually monitored with mass spectroscopy (EI). Evidence for $\text{F}_2\text{BCH}_2\text{F}$ was not found. The products of this reaction have not been characterized. The two reaction exotherms may indicate 1,2-migration, followed by further decomposition. Alternatively, these reactions may occur by completely different processes other than 1,2-migration. Fluorine 1,2-migration has been demonstrated in one system: the reaction of diazomethane with BF_3 in the gas phase at $-40\text{ }^{\circ}\text{C}$.³⁸

Reversible (physical) and irreversible (chemical) heat flows can be deconvoluted using modulated DSC (MDSC) instrumentation.³⁹ The MDSC heating profile for complex **6**, which is representative for the complexes analyzed in this study, is given in Figure 6. The total heat flow (top trace) is the sum of the reversible heat flow (middle trace) and nonreversible heat flow (bottom trace). The nonreversing heat flow scan shows a large exothermic peak ($\Delta H_{\text{rxn}} = -15.7\text{ kcal mol}^{-1}$), presumably due to 1,2-migration. The heats of 1,2-migration (ΔH_{rxn}) are listed in Table 1. The most exothermic rearrangement, ylide- BH_3 (**5**), has a ΔH_{rxn} of $54.7\text{ kcal mol}^{-1}$ or 517 cal g^{-1} , about 1.5 times that of ammonium perchlorate by weight (347 cal g^{-1}).⁴⁰

The reversing heat flow scan for complex **6** shows a much smaller endothermic peak ($\Delta H_{\text{f}} = 0.3\text{ kcal mol}^{-1}$) than the nonreversing heat flow scan. The apparent heats of fusion for the zwitterionic complexes **3–6** (Table 1) were obtained from integration of the reversing heat flow curves. The heats of fusion for these are lower than the heat of fusion of typical organic molecules. For example, benzene ($\Delta H_{\text{f}} = 2.4\text{ kcal mol}^{-1}$)⁴¹ and benzoic acid ($\Delta H_{\text{f}} = 4.1\text{ kcal mol}^{-1}$)⁴¹ all have higher heats of fusion than complexes **3–6**. Since the two processes, reversible and nonreversible heat flow, overlap and the former dominates the thermal analyses, the uncertainties in the reversing component may be significant (Figure 3).

The thermal analyses of solid complexes **3–6** all have strong exothermic signatures. It is reasonable to assume that the exothermicity of these ylide-organoborane complexes is due to the irreversible 1,2-migration from the "ate"-complex, with the exception of complex **3**. In addition, there may be a component of exothermicity due to the complexation of the expelled DMSO and homologated organoborane.

The MDSC (Figure 6) for complex **6** shows a peak onset for nonreversing heat flow of $71.3\text{ }^{\circ}\text{C}$ and a peak onset for reversing heat flow of $74.8\text{ }^{\circ}\text{C}$. All the complexes show an exothermic nonreversing heat flow (ΔH_{rxn}) that slightly precedes an endothermic reversing

(38) Goubeau, J.; Rohwedder, K. H. *Ann.* **1957**, *604*, 168–178.

(39) (a) Brown, M. E. *Introduction to thermal analysis: techniques and applications*; Kluwer Academic Publishers: Boston, 2001. (b) Haines, P. J. *Principles of Thermal Analysis and Calorimetry*; Royal Society of Chemistry: Cambridge, 2002.

(40) Carl, F. *Franklin Inst.* **1940**, *230*, 75.

(41) Hodgman, C. D. *Handbook of Chemistry and Physics*, 31st ed.; Chemical Rubber Publishing Co.: Cleveland, 1949.

(36) Davydov, E.; Vorotnikov, A.; Pariyskii, G.; Zalkov, G. *Kinetic Peculiarities of Solid Phase Reactions*; John Wiley & Sons: New York, 1998.

(37) Wolf, E.; Cammenga, H. K. *Z. Phys. Chem. Neue Fol.* **1977**, *107*, 21–38.

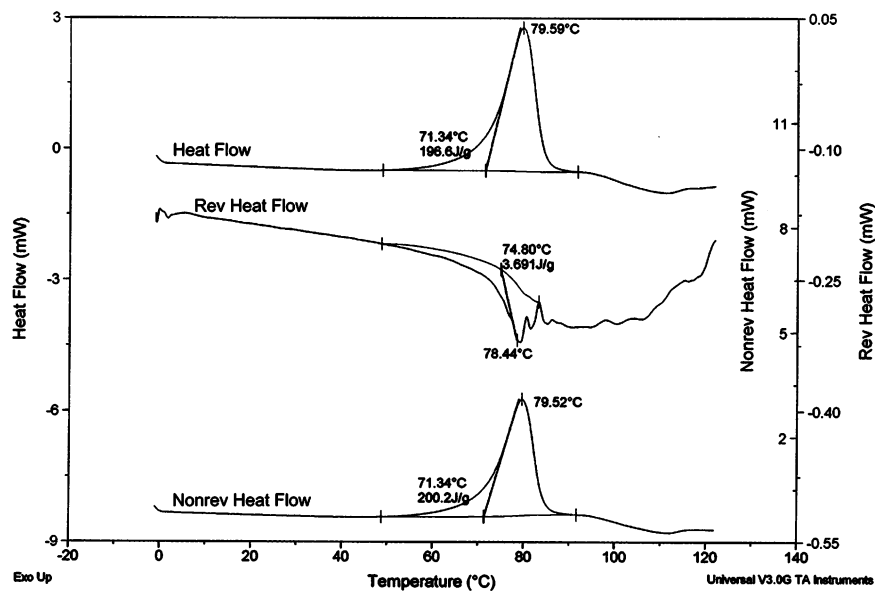
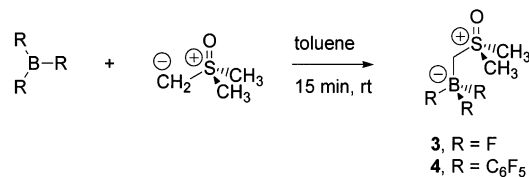


Figure 6. MDSC of complex **6** showing total, reversing, and nonreversing heat flow.

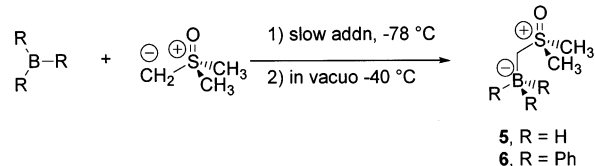
heat flow (ΔH_f). The MDSC data suggest that the solid complexes undergo exothermic 1,2-migration in the solid state that induces further reaction and melting. This implies that the peak onset temperature for the nonreversing heat flow is determined by the chemical stability of the ylide-borane complex and not necessarily an initiated physical “melting point” of the complex followed by reaction. The very low heats of fusion obtained from the reversing heat flows support the hypothesis of a substantial component of the reaction in the solid state. The heat of fusion is a reversible process, but the 1,2-migration is not. If the solid complexes do not melt, but turn liquid via 1,2-migration, then the contribution from reversible heat flow would be expected to be zero. The very low heats of fusion for these zwitterionic complexes suggest this is at least partially true. The peak onset temperatures from the DSC qualitatively establish a reaction onset temperature for 1,2-migration for ylide- BR_3 complexes in the solid state, $\text{R} = \text{C}_6\text{F}_5 > \text{Ph} > \text{H}$. Interestingly, this trend correlates with the measured Lewis acidity of the corresponding boranes C_6F_5 (6.38) $>$ Ph (3.85) $>$ H (3.79).⁴²

Analysis of the Products of Decomposition of Complex 4. In an effort to relate the exotherm of the ylide-borane complex to the 1,2-migration reaction, the decomposition of solid complex **4** was studied. Solid ylide- $\text{B}(\text{C}_6\text{F}_5)_3$ complex (**4**) was heated to 150 °C for 10 min under nitrogen. Oxidation was then carried out in refluxing benzene with 6 equiv of anhydrous trimethylamine-*N*-oxide (TAO)⁴³ for 15 h (Scheme 5). An analysis by GC/MS indicated the presence of pentafluorobenzyl alcohol. Neither pentafluorophenol nor pentafluorophenethyl alcohol were detected. Presumably, the pentafluorophenyl group is less reactive than the pentafluorobenzyl group toward oxidation with TAO. This may explain the preferential formation of pentafluorobenzyl alcohol over pentafluorophenol. Furthermore, the liberated

Scheme 3



Scheme 4



trimethylamine may irreversibly complex with the partially oxidized organoborane, thereby shielding it toward further oxidation to produce pentafluorophenol.

In another experiment, complex **4** was heated at 150 °C for 10 min, dissolved in CDCl_3 , and allowed to evaporate (Scheme 5). Crystals formed over several weeks. The molecular structure of $(\text{C}_6\text{F}_5)_2\text{BCH}_2(\text{C}_6\text{F}_5) \cdot \text{DMSO}$ complex **7** obtained by single-crystal X-ray analysis is shown in Figure 7. Since the product organoborane is highly Lewis acidic, complexation with DMSO in the melt occurs to provide organoborane-DMSO complex **7**. The B–O bond distance of 1.560(3) Å indicates a strong coordination between the sulfoxide oxygen and electrophilic borane. The B–O bond distance can be compared to a complex with homoboradadamantane (B–O 1.668(3) Å), a highly Lewis acidic borane.²⁴ The isolation of this complex **7** indicates that the pentafluorophenyl group of complex **4** (Figure 2) has undergone 1,2-migration. This experiment supports the hypothesis that complex **4** undergoes 1,2-rearrangement in the DSC experiments shown earlier. Since complexes **5** and **6** display similar MDSC traces with an exothermic nonreversing peak preceding an endothermic reversing peak, it is likely that they also undergo 1,2-rearrangement in the solid state.

(42) Farfan, N.; Contreras, R. *J. Chem. Soc., Perkin Trans. 2* **1987**, 771.

(43) Soderquist, J. A.; Najafi, M. R. *J. Org. Chem.* **1986**, *51*, 1330–1336.

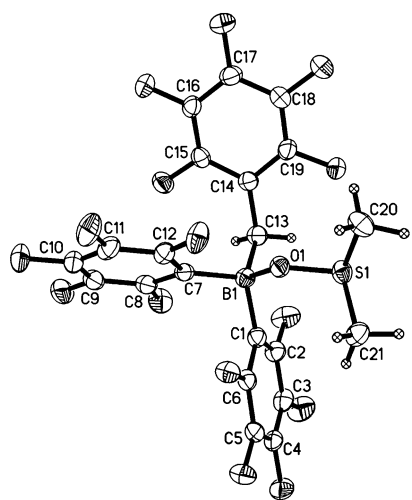
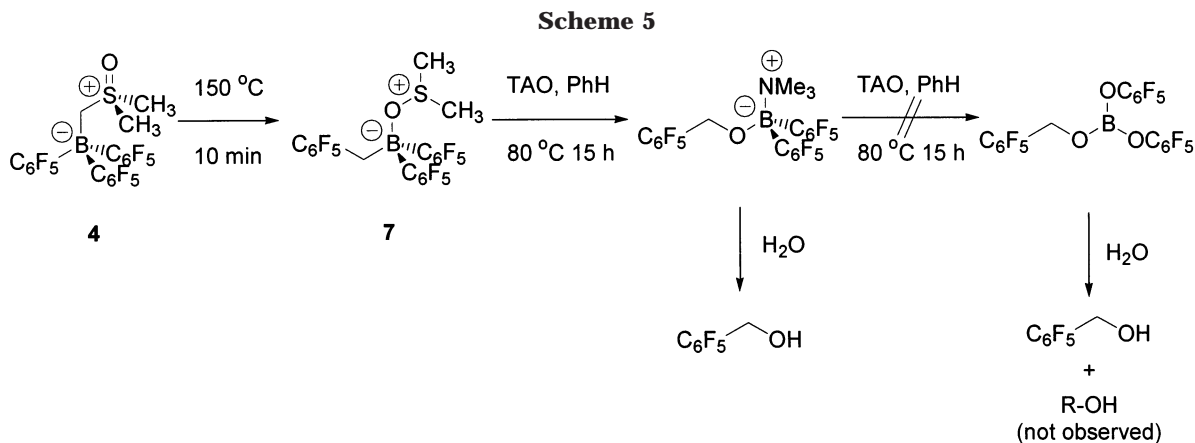


Figure 7. Molecular structure of $(\text{C}_6\text{F}_5)_2\text{BCH}_2(\text{C}_6\text{F}_5)\cdot\text{DMSO}$ (7). Selected bond lengths (Å) and angles (deg): S1–C20 1.783(3), S1–C21 1.780(3), S1–O1 1.561(2), B1–C1 1.647(3), B1–C7 1.647(3), B1–C13 1.634(3), B1–O1 1.560(3), C13–C14 1.507(3); C21–S1–C21 98.09(14), C20–S1–O1 99.48(11), C21–S1–O1 104.71(11), S1–O1–B1 122.84(13), C1–B1–O1 107.39(17), C1–B1–C7 110.00(17), C1–B1–C13 114.36(18), O1–B1–C13 109.77(18), B1–C13–C14 113.19(18).

A proposed reaction coordinate diagram (Figure 8) for complex **4** shows a high activation energy for the 1,2-migration. The activation energy for dissociation of complex **4** to produce tris(pentafluorophenyl)borane and free ylide may be lower. The 1,2-migration initially produces a homologated organoborane and DMSO. The DMSO then coordinates to the organoborane to produce DMSO complex **7**. DMSO has also been shown to weakly coordinate to the less Lewis acidic triethylborane. The complexation between DMSO and the homologated organoboranes in this study is likely.

This study reveals that ylide **1** complexes of strongly Lewis acidic boranes such as $\text{B}(\text{C}_6\text{F}_5)_3$ have higher activation energies toward 1,2-migration. The effects of electron-withdrawing groups attached to boron are twofold. First, the Lewis acidity is increased⁴² and the resulting ylide complex is more stable (Figure 8). Second, electron-withdrawing groups on boron lower the HOMO energy of the migrating group (Figure 4). This is expected to raise the activation energy for 1,2-rearrangement. For example, the fluorine substituents serve to lower the HOMO of the π -system for complex

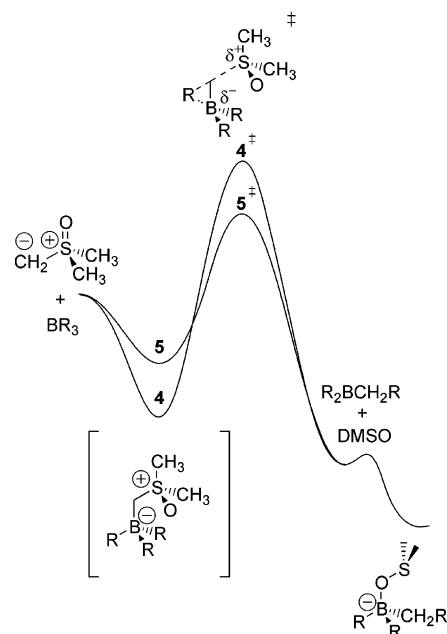


Figure 8. Reaction coordinate diagram for the 1,2-migration reaction of ylide· $\text{B}(\text{C}_6\text{F}_5)_3$ (**4**) ($\text{R} = \text{C}_6\text{F}_5$) and ylide· BPh_3 (**5**) ($\text{R} = \text{Ph}$) and the subsequent coordination of DMSO.

4, which can lead to a higher activation energy barrier for 1,2-migration. Both of these effects combine to raise the activation energy barrier and increase the stability of the complexes. It is not known which one has a greater affect on the transition state energy in the current study.

Conclusion

A series of complexes of dimethylsulfoxonium methylene ylide (**1**) and various organoboranes have been prepared and isolated. Molecular structures, obtained by single-crystal X-ray diffraction, for ylide· BF_3 (**3**) and ylide· $\text{B}(\text{C}_6\text{F}_5)_3$ (**4**) were found to contain geometries with the potential migrating group anti-periplanar to the carbon–sulfur bond. The reaction onset of the solid complexes ylide· BF_3 (**3**), ylide· $\text{B}(\text{C}_6\text{F}_5)_3$ (**4**), ylide· BH_3 (**5**), and ylide· BPh_3 (**6**) were evaluated using DSC and found to correlate to the Lewis acidity of the organoborane. Thus the onset temperature of reaction in the solid state of ylide· BR_3 ($\text{R} = \text{F} > \text{C}_6\text{F}_5 > \text{Ph} > \text{H}$) correlated with the Lewis acidity of the organoborane BR_3 ($\text{R} = \text{F} > \text{C}_6\text{F}_5$

Table 2. Crystal Data and Structure Refinement Parameters for Complexes **3**, **4**, and **7**

	3	4	7
empirical formula	C ₃ H ₈ BF ₃ OS	C ₂₁ H ₈ BF ₁₅ OS	C ₂₁ H ₈ BF ₁₅ OS
fw	159.96	604.14	604.14
temperature (K)	178(2)	158(2)	173(2)
λ (Mo K α) Å	0.71073	0.71073	0.71073
crystal syst	orthorhombic	monoclinic	triclinic
space group	<i>P</i> 2 ₁ 2 ₁ 2 ₁	<i>P</i> 2 ₁ / <i>n</i>	<i>P</i> (<i>ob</i>) 1(<i>obx</i>)
unit cell dimens			
<i>a</i> (Å)	5.5467(4)	18.8527(15)	10.3619(4)
<i>b</i> (Å)	8.1059(5)	13.0080(10)	10.4008(4)
<i>c</i> (Å)	14.4239(10)	19.7288(16)	12.3825(5)
α (deg)	90.0	90.0	102.1170(10)
β (deg)	90.0	115.7860(10)	101.5670(10)
γ (deg)	90.0	90.0	116.5960(10)
<i>V</i> (Å ³)	648.51(8)	4356.4(6)	1098.51(7)
<i>Z</i>	4	8	2
ρ_{calc} (g cm ⁻³)	1.638	1.842	1.826
μ (mm ⁻¹)	0.472	0.292	0.290
<i>F</i> (000)	328	2384	596
cryst size (mm)	0.33 × 0.29 × 0.15	0.40 × 0.35 × 0.26	0.29 × 0.21 × 0.17
diffractometer	Bruker CCD	Bruker CCD	Bruker CCD
θ range (deg)	2.82–28.26	1.25–28.30	2.31–28.29
no. of total/unique data [<i>I</i> > 2 σ (<i>I</i>)]	4197/1533	27 920/10 304	11 880/5195
no. of obsd data	1533	10 304	3954
no. of params	116	768	384
final <i>R</i> 1 ^a	0.0232	0.0420	0.0418
final <i>wR</i> 2 ^b	0.0633	0.1156	0.0976
goodness-of-fit ^c	1.069	1.039	1.035
difference Fourier (e Å ⁻³)	0.252/–0.255	0.417/–0.404	0.470/–0.357

^a $\sum ||F_o| - |F_c|| / \sum |F_o|$. ^b $[\sum (w(F_o^2 - F_c^2)^2) / \sum (w(F_o^2)^2)]^{1/2}$. ^c $[\sum (w(F_o^2 - F_c^2)^2) / (N_{\text{ref}} - N_{\text{var}})]^{1/2}$.

> Ph > H). Thermal analysis using DSC was also used to obtain the ΔH_{rxn} for 1,2-migration for complexes **4**–**6**. The heats of reaction for the ylides·BR₃ complexes (R = H > C₆F₅ > Ph > F) correlate with heats of reaction estimated with average bond dissociation energies (R = H > C₆F₅ ≈ Ph > F).

Experimental Section

General Considerations. All reactions were carried out in anhydrous solvents under N₂. Toluene was dried over calcium hydride, and tetrahydrofuran (THF) was obtained by passing through an alumina column under Ar. Solutions of ylide **1** in THF³⁰ and toluene²² were synthesized as previously reported. Triphenylborane (Aldrich) was sublimed (0.05 mmHg, temp) and BF₃·OEt₂ (Aldrich, 99% redistilled) was distilled before use. Anhydrous trimethylamine-*N*-oxide was prepared from trimethylamine-*N*-oxide dihydrate (Aldrich).⁴³ THF was dried by passing through an alumina column under Ar. Tris(pentafluorophenyl)borane (95% Aldrich) was used as received.

Thermal Analysis: MDSC and DSC. Differential scanning calorimetry (DSC) was recorded on a Du Pont 910 DSC instrument with Al₂O₃ as an internal reference standard and a heating rate of 5 °C min⁻¹. MDSC was obtained on a DSC 2920 instrument with a heating rate of 0.2 °C min⁻¹, MDSC heating profile of 0.313 °C and 60 s period, and under N₂ flow (50 cm³ min⁻¹). Samples were weighed (5–8 mg) into crimped aluminum pans for complexes **3**, **4**, and **6**. Complex **5** was weighed out in smaller amounts (1.5 mg) due to its violent decomposition.

X-ray Crystallography: Data Collection and Refinement. Single crystals of the complexes **3**, **4**, and **7** were grown from MeOH/H₂O, toluene, and CDCl₃, respectively. Diffraction data were obtained on a Bruker CCD platform diffractometer. The SMART⁴⁴ program package was used to determine the unit-cell parameters and for data collection (30 s/frame scan time for a hemisphere of diffraction data). The raw frame data

were processed using SAINT⁴⁴ and SADABS⁴⁵ to yield the reflection data file. Subsequent calculations were carried out using the SHELXTL⁴⁵ program. The structure was solved by direct methods and refined on *F*² by full-matrix least-squares techniques. The analytical scattering factors⁴⁶ for neutral atoms were used throughout the analysis. Hydrogen atoms were located from a difference Fourier map and refined (*x*, *y*, *z* and *U*_{iso}). All details of the crystal, data collection, and refinement parameters are summarized in Table 2.

Dimethylsulfoxonium Methylide·Trifluoroborane (**3**).

To a solution of ylide **1** (0.4 M in toluene, 10 mL, 4 mmol) was gradually added freshly distilled BF₃·OEt₂ (0.5 mL, 4 mmol, 1 equiv). The reaction mixture was stirred for 12 h at room temperature. The precipitate was filtered and recrystallized three times from 1:1 EtOH/H₂O to yield pale brown crystals (0.24 g, 37% yield): mp 167.4–168.2 °C (lit³¹ mp 245–270 °C); IR (KBr) ν_{max} 3037.7, 2939.7, 1225.3, 1039.4, 989.1, 575.8 cm⁻¹; ¹H NMR (500 MHz, MeOH-*d*₄/d₂O, 1:1) δ 3.59 (s, 6H), 2.97 (s, 2H); ¹⁹F NMR (376 MHz, MeOH-*d*₄/d₂O, 1:1) δ 134.5 (q, *J* = 44.7 Hz); ¹³C NMR (125 MHz, MeOH-*d*₄/d₂O, 1:1) δ 40.7 (q, *J* = 1.9 Hz); ¹¹B NMR (160 MHz, MeOH-*d*₄/d₂O, 1:1) δ –23.0 (q, *J* = 45.0 Hz); HRMS (CI/isobutane) *m/z* calcd for BC₃F₃H₈OS (M – F)⁺ 141.0358, found 141.0357. Anal. Calcd for C₃H₈SBF₃O: C, 22.50; H, 5.04. Found: C, 22.62; H, 4.97.

Dimethylsulfoxonium Methylide·Tris(pentafluorophenyl)borane (**4**).

A stirred solution of tris(pentafluorophenyl)borane (66 mg, 0.13 mmol) in degassed toluene (3.0 mL) was treated with ylide **1** (0.64 M in toluene, 0.25 mL, 0.16 mmol). After stirring 45 min, the solution was concentrated under reduced pressure to yield a glassy solid. The material was dissolved in CHCl₃ (10 mL), and hexane (10 mL) was added. The white cubic crystals formed were filtered (63 mg, 82% yield): mp 140.7–147.9 °C; IR (KBr) ν_{max} 1638.2, 1518.6, 1465.0, 1087.9, 979.3 cm⁻¹; ¹H NMR (400 MHz, tol-*d*₆) δ 3.25 (br s, 2H), 1.49 (s, 6H); ¹⁹F NMR (376 MHz, tol-*d*₆) δ 133.2 (m, 2F), 158.8 (t, *J* = 20.4 Hz, 1F), 164.3 (m, 2F); ¹¹B NMR (160

(45) Sheldrick, G. M. *SADABS*; Bruker Analytical X-Ray Systems, Inc.: Madison, WI, 1999.

(46) *International Tables for X-Ray Crystallography*; Kluwer Academic Publishers: Dordrecht, 1992; Vol. C.

(44) *SMART Software Users Guide*, Version 5.1; Bruker Analytical X-Ray Systems, Inc.: Madison, WI, 1999.

MHz, *tol-d*₈, 100 °C) δ -16.3 (s); DSC (exotherm) 150.0 °C (94.2 J/g); HRMS (FAB/CI) *m/z* calcd for C₁₅H₈BSF₁₀O (M - C₆F₅)⁺ 437.0224, found 437.0229. Anal. Calcd for C₂₁H₈BSF₁₅O: C, 41.75; H, 1.33. Found: C, 41.72; H, 1.38.

Dimethylsulfoxonium Methylide-Borane (5).³⁴ Ylide **1** (0.61 M in THF, 1.4 mL, 1.0 mmol) was added dropwise over 10 min to a suspension of BH₃·SMe₂ (1.0 M in THF, 1 mL, 1.0 mmol) in THF (5 mL) at -78°. The white precipitate was filtered cold, washed with hexane, and dried in vacuo to afford a white solid (0.14 g, 100% yield): mp 57.8–58.8 °C (dec); DSC (exotherm) 66.3 °C, 67.4 °C; IR (KBr) ν_{\max} 3021.9, 2920.1, 2283.6, 1204.2, 1132.3, 1034.1 cm⁻¹; ¹¹B NMR (160 MHz, DMF, 0 °C) δ -31.2 (s).

Dimethylsulfoxonium Methylide-Triphenylborane (6). Ylide **1** (0.61 M in THF, 0.70 mL, 0.49 mmol) was added dropwise over 10 min to a stirred suspension of Ph₃B (0.12 g, 0.49 mmol) in degassed THF (5 mL) at -78 °C. The solvent was removed in vacuo over 2 days at -40 °C to yield a white solid (0.14 g, 100% yield): mp 81.0–88.1 °C; DSC (exotherm) 92.0 °C (196.9 J/g); IR (KBr) ν_{\max} 3058.3, 3013.2, 2912.4, 1228.3, 710.5 cm⁻¹; ¹¹B NMR (160 MHz, *tol-d*₈, -20 °C) δ -10.3 (s).

Bis(pentafluorophenyl) 2,3,4,5,6-Pentafluorobenzylborane-DMSO Complex (7). Ylide·B(C₆F₅)₃ complex **4** (10 mg) was heated to 150 °C in an NMR tube for 10 min and cooled to room temperature, and CDCl₃ (0.5 mL) was then

added. The solution was allowed to evaporate slowly at room temperature over several weeks. The colorless crystals were separated from a yellow oily residue: ¹H NMR (500 MHz, CDCl₃) δ 2.89 (s, 6H), 2.58 (s, 2H); ¹⁹F NMR (376 MHz, CDCl₃) δ -133.6 (dd, *J* = 23.9, 8.7 Hz, 4F), -143.9 (dd, *J* = 22.7, 7.2 Hz, 2F), -157.1 (t, *J* = 20.3 Hz, 2F), -162.0 (t, *J* = 21.2 Hz, 1F), -163.7 (dt, *J* = 2.2, 7.8 Hz, 4F), -165.2 (dt, *J* = 21.6, 6.4 Hz, 2F); ¹¹B NMR (160 MHz, CDCl₃) δ 3.9 (s); HRMS (FAB/CI) *m/z* calcd for C₁₉H₂BF₁₅ (M - C₂H₆SO)⁺ 526.0014, found 526.0008.

Acknowledgment. We thank the Chemistry Division of the National Science Foundation for financial support of this work, Dr. Joe Ziller for X-ray crystallographic data, and Dr. Marvin Grzys (TA Instruments, 109 Lukens Dr., New Castle, DE 19720) for generously providing the MDSC data for complexes **3–6**.

Supporting Information Available: MDSC traces for complexes **3–6**. Tables of atomic coordinates, all bond distances and angles, and anisotropic thermal parameters for compounds **3**, **4**, **7**, and MeB(OH)₂. This material is available free of charge via the Internet at <http://pubs.acs.org>.

OM0208568